Quantitative Analysis of Factors Contributing to Urban Heat Island Intensity

YOUNG-HEE RYU AND JONG-JIN BAIK

School of Earth and Environmental Sciences, Seoul National University, Seoul, South Korea

(Manuscript received 7 May 2011, in final form 23 September 2011)

ABSTRACT

This study identifies causative factors of the urban heat island (UHI) and quantifies their relative contributions to the daytime and nighttime UHI intensities using a mesoscale atmospheric model that includes a single-layer urban canopy model. A midlatitude city and summertime conditions are considered. Three main causative factors are identified: anthropogenic heat, impervious surfaces, and three-dimensional (3D) urban geometry. Furthermore, the 3D urban geometry factor is subdivided into three subfactors: additional heat stored in vertical walls, radiation trapping, and wind speed reduction. To separate the contributions of the factors and interactions between the factors, a factor separation analysis is performed. In the daytime, the impervious surfaces contribute most to the UHI intensity. The anthropogenic heat contributes positively to the UHI intensity, whereas the 3D urban geometry contributes negatively. In the nighttime, the anthropogenic heat itself contributes most to the UHI intensity, although it interacts strongly with other factors. The factor that contributes the second most is the impervious-surfaces factor. The 3D urban geometry contributes positively to the nighttime UHI intensity. Among the 3D urban geometry subfactors, the additional heat stored in vertical walls contributes most to both the daytime and nighttime UHI intensities. Extensive sensitivity experiments to anthropogenic heat intensity and urban surface parameters show that the relative importance and ranking order of the contributions are similar to those in the control experiment.

1. Introduction

The urban heat island (UHI) is the most well documented example of anthropogenic climate modification (Arnfield 2003). Numerous studies have reported that the urban air temperature can be 1°–3°C higher than the rural or surrounding air temperature on average (e.g., Oke 1981; Morris et al. 2001; Bottyan and Unger 2003; Kim and Baik 2004; Grimmond 2007). Some studies have reported cases of very strong UHI intensity (e.g., Klysik and Fortuniak 1999; Fung et al. 2009). The UHI intensity is strongly related both to external influences (e.g., climate, weather, and season) and to the intrinsic characteristics of a city (e.g., city size, building density, and land-use distribution) (Oke 1982). In terms of meteorological conditions, calm, dry, and clear nights near the center of anticyclones are favorable for strong UHI intensity (Gedzelman et al. 2003).

Several factors that cause UHI have been proposed in the literature (e.g., Oke 1982; Grimmond 2007; Rizwan et al. 2008; Hidalgo et al. 2008). It is known that the UHI is caused by complex interactions among many factors, including decreased urban albedo (ALB), increased thermal mass per unit area, increased city roughness, increased anthropogenic heat released from buildings and vehicles, and decreased evaporative areas (fewer trees and more impervious materials) (Taha et al. 1988). Even though these causative factors have long been established, their relative importance remains uncertain. Extensive efforts have been devoted to find relationships between the UHI intensity and specific urban surface parameters, such as surface albedo, thermal properties of surface materials, sky-view factor, and vegetation fraction, but quantifying the relative contributions of each causative factor to the UHI intensity has received less attention.

This study aims to understand and quantify the relative contributions of causative factors and interactions between the factors to the UHI intensity. Following previous studies, the causative factors are recategorized into three main factors: anthropogenic heat, impervious

Corresponding author address: Jong-Jin Baik, School of Earth and Environmental Sciences, Seoul National University, Seoul 151-742, South Korea.
E-mail: jjbaik@snu.ac.kr

DOI: 10.1175/JAMC-D-11-098.1

TABLE 1. Suggested causative factors of the UHI. The main factors are denoted by F_1, F_2, and F_3, and the subfactors are denoted by G_1, G_2, and G_3.

Causative factors	Description
Anthropogenic heat F_1	Additional heat released by human activities
Impervious surfaces F_2	Reduction in surface moisture availability and increase in thermal inertia of urban surface materials
Three-dimensional urban geometry F_3	
Additional heat stored in vertical walls G_1	Additional surfaces in the vertical (walls) that are able to absorb and store heat
Radiation trapping G_2	Increase in absorption of shortwave radiation and decrease in loss of longwave radiation within an urban canyon
Wind speed reduction G_3	Wind speed reduction above and within an urban canopy layer due to the existence of buildings

surfaces, and three-dimensional (3D) urban geometry. The 3D urban geometry factor is further examined by subdividing it into three subfactors: additional heat stored in vertical walls, radiation trapping, and wind speed reduction. This is a new classification of causative factors of the UHI, as described in Table 1. The causative factors are discussed further in the following section.

A few studies have quantitatively investigated the roles of causative factors in UHI intensity. Martilli (2002) examined the effects of thermal and mechanical factors on the urban boundary layer structure using the factor separation method and showed that the thermal factor is more important than the mechanical factor in contributing to the nighttime UHI intensity. In that study, several factors that contribute to thermal effects were integrated into a single factor, rather than separated, and therefore only the total thermal effects were examined. Kusaka and Kimura (2004) examined the individual effects of anthropogenic heat, a large heat capacity (HCP) particularly due to the existence of walls, and a small sky-view factor of an urban canyon on the nighttime UHI intensity. That study highlighted the effect of anthropogenic heat on the nighttime UHI intensity, but the effects of impervious surfaces, wind speed reduction, and interactions between the factors were not considered. Tokairin et al. (2006) performed a factor separation analysis to examine the effects of heat release from building surfaces and of wind speed reduction by the drag of buildings on the UHI intensity. They concluded that the contribution of the heat released from building surfaces is more dominant than that of the wind speed reduction in the urban area. Not all factors were considered separately in their study, however.

Previous quantitative studies on the relative contributions of causative factors to the UHI intensity have been limited to certain aggregated factors, without sufficiently separating their contributions. To separate and quantify the relative contributions of the individual factors listed in Table 1 and their interactions to the UHI intensity, a factor separation analysis is performed. In this study, unlike other studies that focused mainly on the nighttime UHI intensity, both the daytime and nighttime UHI intensities are analyzed.

To take into account the relevant physical processes that occur in urban areas and to examine the 3D urban geometry effect on the UHI intensity, we employ a mesoscale atmospheric model that includes a single-layer urban canopy model. Traditional slab models have some limitations for studying the UHI because the models do not consider 3D urban geometry. In other words, slab models are not able to simulate explicitly additional heat stored in vertical walls, radiation trapping, wind speed reduction, and interactions among these factors. Therefore, an urban canopy model is required to understand the quantitative contributions of the factors to the UHI intensity in detail.

The relative contributions of each factor to the UHI intensity are not the same in different climates or city features (Mirzaei and Haghighat 2010). For example, the contribution of anthropogenic heat to the urban energy balance depends largely on latitude and the season of the year (Shahmohamadi et al. 2010). To simplify environmental and meteorological conditions, we consider an idealized urban environment: a midlatitude city surrounded by a cropland/woodland mosaic in summertime with fair weather. No initial background wind is considered. Note that in this study a relatively strong urban-breeze circulation (or UHI-induced circulation) is generated in the daytime, in response to the temperature gradient associated with the UHI between the urban and rural areas. Thus, even though an initial background wind is not considered, the relatively strong internally generated wind blows over the urban area. This study aims to understand the influences of the intrinsic characteristics of a city (e.g., anthropogenic heat intensity, roof fraction (RFR), and heat capacity of urban surface materials) on the UHI intensity rather than the influences of meteorological conditions.

Section 2 presents the experimental design, the causative factors, and the factor separation method. In section 3,

the results are presented and discussed. A summary and conclusions are given in section 4.

2. Experimental design, causative factors, and factor separation

a. Mesoscale atmospheric model and experimental design

The Advanced Research Weather Research and Forecasting (WRF) model (Skamarock et al. 2008) is employed as a mesoscale atmospheric model. Physical parameterization options used in this study are the Dudhia shortwave radiation scheme (Dudhia 1989), the Rapid Radiative Transfer Model longwave radiation scheme (Mlawer et al. 1997), the ''Noah'' land surface model (Noah LSM; Chen and Dudhia 2001), the Yonsei University planetary boundary layer scheme (Hong et al. 2006), and the Purdue–Lin cloud microphysics scheme (Chen and Sun 2002).

As an urban module, the Seoul National University Urban Canopy Model (SNUUCM; Ryu et al. 2011) is adopted. The urban canopy model is a single-layer urban canopy model and represents an urban canopy as an urban canyon and two separate buildings. The urban canyon is treated as a single layer in the model, and the canyon air temperature is calculated at a representative level, that is, at the displacement height that is set equal to 0.65 times the mean building height. The model parameterizes many important physical processes that occur in an urban canopy: absorption and reflection of shortwave and longwave radiation, exchanges of turbulent energy and water between surfaces (roof, two facing walls, and road) and adjacent air, and conductive heat transfer in substrates. The SNUUCM is validated by using datasets obtained at two European urban sites and shows good performances in reproducing canyon air temperatures, surface temperatures (roof, walls, and road), and urban-averaged net radiation, sensible heat flux, latent heat flux, and storage heat flux for both sites (Ryu et al. 2011). For example, the root-mean-square error of sensible heat flux for the sites is 50–60 W m^{-2} for the overall period. In particular, the wall temperatures that exhibit different diurnal variations of sunlit and shaded walls depending on canyon orientation are well reproduced. The SNUUCM is implemented in the WRF model by coupling it to the Noah LSM in a tile approach (hereinafter called the coupled WRF–SNUUCM model). In other words, a built-up area in an urban area is represented by the SNUUCM, a natural area in an urban area is represented by the Noah LSM, and the output energy fluxes are then area-weighted for urban-averaged energy fluxes.

TABLE 2. Urban surface parameters used in the control and sensitivity experiments.

Parameters	Control expt	Sensitivity expt
Area fractions		
Built-up area	0.8	0.8
Natural area	0.2	0.2
Geometric parameters		
Mean building height (m)	15	15
Canyon orientation (°)	180	180
Canyon aspect ratio	1.0	0.5 ($H/W \times 0.5$) 2.0 ($H/W \times 2.0$)
Roof fraction	0.5	0.4 (RFR × 0.8) 0.6 (RFR × 1.2)
$z_{0m}/z_{0\theta}$ for canyon air	10^2	10^2
Roof, wall, and road properties		
Albedo	0.16	0.12 (ALB × 0.75) 0.20 (ALB × 1.25)
Emissivity	0.95	0.95
Heat capacity (MJ m^{-3} K^{-1})	1.4	1.12 (HCP × 0.8) 1.68 (HCP × 1.2)
Thermal conductivity (W m^{-1} K^{-1})	0.8	0.64 (TCD × 0.8) 0.96 (TCD × 1.2)
$z_{0m}/z_{0\theta}$ (only for roof and road)	10^2	10^2

Two-dimensional idealized experiments are conducted using the coupled WRF–SNUUCM model. The latitude is set to 30°N. The Coriolis force is excluded. The domain size is 200 km in the x direction and 6 km in the z direction with a Rayleigh damping layer of 2 km. The horizontal grid interval is 500 m. The vertical grid interval is stretched with height, starting from 60 m above the surface. The lowest model level is therefore 30 m. There are 65 vertical layers in total and 30 vertical layers below 2 km with a grid interval of the 30th layer of 73 m. The periodic boundary condition is applied at lateral boundaries. The lapse rate of initial potential temperature is 5 K km^{-1}, and the initial potential temperature near the surface is 298.15 K. The initial relative humidity is constant (30%) from the surface to $z = 4$ km and then decreases linearly with height to $z = 6$ km (10%). The time step is 2 s. The model is integrated for 36 h starting from 0500 LST 20 June 2008 (the year has no meaning). The last 24 h of simulation data are analyzed. The size of a city is 20 km, and its center is located at the center of the model domain.

Values of urban surface parameters in the SNUUCM used in the control and sensitivity experiments are given in Table 2. Note that all albedos of the roof, walls, and road are set to be the same and that the albedo of the rural area is also the same (=0.16). The land-use/land-cover (LULC) type of the rural area is a cropland/woodland mosaic, and the same LULC type is applied to the natural area of the urban area. The vegetation fraction of the natural areas (both the rural and urban

areas) is set to 0.6, and the soil type is loamy sand. The initial soil moisture content (volume of water per volume of soil) and soil temperature are set to 0.25 and 20°C, respectively.

b. Causative factors

Anthropogenic heat F_1 is additional heat released by human activities and likely increases air temperature near the surface. Many researchers have emphasized the important role of anthropogenic heat in the UHI intensity, indicating a temperature rise of 1°–2°C in summertime and a rise of 2°–3°C in wintertime (Ichinose et al. 1999; Kondo and Kikegawa 2003; Fan and Sailor 2005; Ohashi et al. 2007).

The two factors originally suggested by Oke (1982)—reduction in surface moisture availability and increase in thermal inertia of urban surface materials—are integrated into the impervious-surfaces F_2 factor. The two factors arise from the fact that pervious or natural surfaces of small thermal inertia (e.g., grass, crops, trees, and soil) are replaced by impervious or artificial surfaces of large thermal inertia (e.g., concrete, asphalt, and bricks) in urban areas. The thermal properties such as heat capacity and thermal conductivity (TCD) of artificial surfaces can be similar to those of natural surfaces when natural surfaces are wet (Runnalls and Oke 2000). In this study, the large thermal inertia of impervious materials means a high capability to store heat, which is closely related to the low moisture availability of impervious materials as well as the thermal properties such as heat capacity and thermal conductivity. Because of the low moisture availability of impervious materials, the majority of available net radiation is converted into sensible heat flux and storage heat flux rather than into latent heat flux. The large thermal inertia of artificial surfaces and fewer natural surfaces in urban areas have been considered to be the most significant causes of the UHI (Velazquez-Lozada et al. 2006). The large storage heat of impervious materials in the daytime and the positive sensible heat flux during several hours after sunset are responsible for the nighttime UHI, as mentioned by Kusaka and Kimura (2004).

The 3D urban geometry F_3 is a distinctive characteristic of cities, resulting from the existence of buildings. Among the 3D urban geometry subfactors (G_1, G_2, and G_3), the additional heat stored in vertical walls G_1 has received less attention than others. One can expect that the surface, which is able to absorb and store heat, increases with increasing building height. Kusaka and Kimura (2004) stated that this effect due to the walls is roughly equivalent to the increase in heat capacity of surface materials. By conducting an experiment without vertical walls, Dupont and Mestayer (2006) stressed that the storage heat flux decreases in the daytime and that the sensible heat flux increases in the daytime and decreases in the nighttime as compared with the results of an experiment with vertical walls. Thus, the G_1 factor can contribute positively to the nighttime UHI intensity. Unlike the G_1 factor, the radiation trapping G_2 has been well documented in the literature (e.g., Terjung and Louie 1973; Arnfield 1982; Johnson et al. 1991; Mills 1997; Masson 2000; Kusaka et al. 2001; Martilli et al. 2002). The incoming shortwave radiation is absorbed more by the surfaces within an urban canyon because of the multiple reflection of shortwave radiation, thus decreasing effective canyon albedo. The small sky-view factor due to vertical walls reduces outgoing longwave radiation from an urban canyon, thus reducing surface cooling within an urban canyon. The wind speed reduction G_3 occurs above and within an urban canopy layer. The mean wind speed over urban canopies is usually reduced because of the drag caused by buildings, and because of the weak wind the warm air over urban areas tends to stagnate. In comparison with wind speed in rural areas at the same height, wind speed within urban canopies also can be reduced, thus reducing surface cooling because of the reduced turbulence within urban canopies (Oke 1987). Therefore, canyon air temperature can be higher than rural air temperature at the same height.

c. Factor separation

The factor separation method proposed by Stein and Alpert (1993) is used to examine the contributions of individual factors and their interactions. To accomplish this for the main factors, eight experiments are designed (Table 3). Table 4 summarizes the methods of calculating the contributions of the factors and their interactions and the mechanisms leading to the contributions from the experiments. For the subfactors, Table 5 provides corresponding subexperiments, and Table 6 presents calculation methods and the mechanisms leading to the contributions. The f and g in Table 4 and Table 6 represent the area-averaged values of air temperatures at 2 m for each experiment for the main factors and subfactors, respectively. Note that the F_2 factor is inherently included in the subexperiments to avoid an unrealistic situation. In other words, the urban surface materials are set to impervious materials in the subexperiments. Therefore, a detailed examination of the 3D urban geometry effect includes the interaction between the F_2 and F_3 factors $\hat{f}_{23}$.

In this study, anthropogenic heat is directly added to the urban-averaged sensible heat flux. In the original SNUUCM, anthropogenic heat is added to the canyon air temperature equation. It is not possible to add

TABLE 3. Experiments designed for the factor separation analysis for the main factors. The "O" indicates that the factor is included, and the "X" indicates that the factor is excluded.

Expt	Anthropogenic heat F_1	Impervious surfaces F_2	3D urban geometry F_3
f_0	X	X	X
f_1	O	X	X
f_2	X	O	X
f_3	X	X	O
f_{12}	O	O	X
f_{13}	O	X	O
f_{23}	X	O	O
f_{123}	O	O	O

anthropogenic heat to a flat surface with the original method (e.g., f_1 and f_{12} experiments), however. We tested the two methods and compared the results, and we found that the difference in daily mean air temperature at 2 m is 0.17°C in the f_{123} experiment. We then adopt the alternative method of adding anthropogenic heat to the urban-averaged sensible heat flux. The anthropogenic heat that is estimated on the basis of the energy consumption statistics data in Lee et al. (2009) is used in this study. The temporal profile of the anthropogenic heat is adopted from that of the summertime anthropogenic heat averaged over the Gyeong-In region of South Korea that includes Seoul. The minimum, maximum, and 24-h-average anthropogenic heat fluxes in the control experiment are 24 W m^{-2} at 0500 LST, 53 W m^{-2} at 1900 LST, and 41 W m^{-2}, respectively.

To examine the impervious-surfaces effect, the impervious materials of the buildings and the road are replaced by pervious materials in several experiments (f_0, f_1, f_3, and f_{13} experiments). The LULC and soil types of the pervious surfaces are set equal to those of the rural area, that is, cropland/woodland mosaic and loamy sand, respectively. The radiation processes such as absorption and reflection are treated using the SNUUCM, but sensible heat fluxes, latent heat fluxes, soil temperatures, and soil moistures for the pervious surfaces are calculated using the Noah LSM.

When the 3D urban geometry factor is included, both the buildings and the urban canyon are considered. When the factor is excluded, however, the surface is regarded as a flat surface and the roughness length in the urban area is set equal to that in the rural area (=0.2 m). In the subexperiments, the G_1 effect is examined by changing the thermal properties of the walls, that is, the heat capacity and thermal conductivity. When the G_1 factor is excluded, the values of the heat capacity and thermal conductivity of the walls are set to be very small (to the values of air at room temperature). Therefore, in this case, there is very little storage heat in the walls. To examine the radiation-trapping G_2 effect, the approach of Kusaka and Kimura (2004) is adopted. The walls are set as transparent to shortwave and longwave radiation, and the road receives the same shortwave and longwave radiation as the roof. The walls absorb, reflect, and emit no radiation. The wind speed reduction G_3 primarily results from the existence of buildings in urban areas. In mesoscale atmospheric models, however, buildings are not explicitly resolved in both the horizontal and vertical directions. Instead, the building effect is represented by roughness length. It is expected that if the roughness length is large then high-rise buildings are present. Therefore, when the G_3 factor is included, the roughness length in the urban area is set to be a large value (=1.5 m). When the G_3 factor is excluded, however, the roughness length in the urban area is set equal to that in the rural area (=0.2 m). In addition, the canyon wind speed, which is generally smaller than the wind speed at the reference level (the lowest model level), is assumed to equal the wind speed at the reference level. Hence, the wind speed reduction within the urban canyon is also ignored.

3. Results and discussion

a. Control experiment

Air temperatures at 2 m that are calculated in the WRF model are averaged over all the grids in the city for each experiment, and daytime and nighttime average

TABLE 4. Contributions of the main factors and their interactions, calculation method, and the mechanisms leading to the contributions.

Symbol	Calculation method	Mechanism
$\hat{f}_0$	f_0	Nonurban
$\hat{f}_1$	$f_1 - f_0$	Anthropogenic heat
$\hat{f}_2$	$f_2 - f_0$	Impervious surfaces
$\hat{f}_3$	$f_3 - f_0$	3D urban geometry
$\hat{f}_{12}$	$f_{12} - (f_1 + f_2) + f_0$	Interaction between anthropogenic heat and impervious surfaces
$\hat{f}_{13}$	$f_{13} - (f_1 + f_3) + f_0$	Interaction between anthropogenic heat and 3D urban geometry
$\hat{f}_{23}$	$f_{23} - (f_2 + f_3) + f_0$	Interaction between impervious surfaces and 3D urban geometry
$\hat{f}_{123}$	$f_{123} - (f_{12} + f_{13} + f_{23}) + (f_1 + f_2 + f_3) - f_0$	Interaction between all main factors

TABLE 5. As in Table 3, but for the subfactors.

Expt	Additional heat stored in vertical walls G_1	Radiation trapping G_2	Wind speed reduction G_3
g_0 (=f_2)	X	X	X
g_1	O	X	X
g_2	X	O	X
g_3	X	X	O
g_{12}	O	O	X
g_{13}	O	X	O
g_{23}	X	O	O
g_{123} (=f_{23})	O	O	O

UHI intensities are calculated. Here, daytime and nighttime averages are defined as the value averaged over the period from 1200 to 1700 LST and 0000 to 0500 LST, respectively. Figures 1 and 2 show the contributions of the factors and their interactions to the daytime and nighttime UHI intensities, respectively. The sum of all contributions is 2.15°C in the daytime and 9.06°C in the nighttime. These values are identical to the daytime and nighttime UHI intensities (i.e., f_{123} experiment − f_0 experiment). In the f_0 experiment, the daytime average temperature is 31.9°C and the nighttime average temperature is 18.4°C. The daytime and nighttime UHI intensities are strong but are within the range observed in real cities [for example, by Kim and Baik (2002) and Giridharan et al. (2007) for the daytime UHI intensity and Klysik and Fortuniak (1999) and Fung et al. (2009) for the nighttime UHI intensity]. Note that the urban surface parameters that are based on those of highly developed urban areas are applied to all of the grids in the city, and this is to some extent responsible for the strong UHI intensities.

In the daytime, the impervious surfaces contribute most to the UHI intensity (2.10°C/2.15°C × 100% = 98%). As pointed out by Taha (1997), the impervious-surfaces factor is a major contributor to the daytime UHI mainly because of the low evapotranspiration rate. A number of observational studies have reported that vegetation in urban areas can decrease air temperatures by ~1°C in the daytime (e.g., Giridharan et al. 2008; Zoulia et al. 2009; Bowler et al. 2010). The anthropogenic heat contributes positively to the daytime UHI intensity (36%), but the 3D urban geometry contributes negatively to the daytime UHI intensity (−24%). The daytime UHI intensity decreases because of the existence of buildings. This result is consistent with that of Dupont and Mestayer (2006) who demonstrated that sensible heat flux increases in the daytime when the effects of walls are not accounted for. Giridharan et al. (2007) and Kruger et al. (2011) found that less obstruction of the sky arising from low-rise buildings—that is, higher sky-view factor—leads to higher air temperature in the daytime. The contribution of the interaction between the F_1 and F_2 factors is negative (−14%). This implies that the anthropogenic heat emitted to the atmosphere is partly converted into the storage heat of the impervious materials. The contribution of the interaction between the F_1 and F_3 factors is 7%. The contribution of the interaction between the F_2 and F_3 factors is negligible (1%). The contribution of the interaction between all three main factors $\hat{f}_{123}$ is negative and small (−4%).

Figures 1 and 2 also present the contributions of the subfactors. In the daytime, the additional heat stored in vertical walls contributes negatively ($\hat{g}_1 = -0.83$°C) as expected. Because of the increased surface areas, a considerable amount of heat is additionally stored in the walls, thus giving the negative contribution. In the daytime, shortwave radiation is absorbed more in the g_2 experiment than in the g_0 experiment because of the radiation trapping. The urban-averaged albedo is 0.12 in the g_2 experiment and 0.16 in the g_0 experiment. Therefore, $\hat{g}_2$ is positive in the daytime (0.14°C). In the daytime, the G_3 factor decreases air temperature near the surface in the urban area ($\hat{g}_3 = -0.77$°C). The contributions of the G_3 factor to the daytime mean wind speed at 10 m and sensible heat flux are −1.7 m s^{-1} and −81.8 W m^{-2}, respectively. Because the wind speed is reduced, the sensible heat flux from the urban area also decreases. This is consistent with the results of Atkinson

TABLE 6. As in Table 4, but for the subfactors.

Symbol	Calculation method	Mechanism
$\hat{g}_0$	g_0	No 3D urban geometry
$\hat{g}_1$	$g_1 - g_0$	Additional heat stored in vertical walls
$\hat{g}_2$	$g_2 - g_0$	Radiation trapping
$\hat{g}_3$	$g_3 - g_0$	Wind speed reduction
$\hat{g}_{12}$	$g_{12} - (g_1 + g_2) + g_0$	Interaction between additional heat stored in vertical walls and radiation trapping
$\hat{g}_{13}$	$g_{13} - (g_1 + g_3) + g_0$	Interaction between additional heat stored in vertical walls and wind speed reduction
$\hat{g}_{23}$	$g_{23} - (g_2 + g_3) + g_0$	Interaction between radiation trapping and wind speed reduction
$\hat{g}_{123}$	$g_{123} - (g_{12} + g_{13} + g_{23}) + (g_1 + g_2 + g_3) - g_0$	Interaction between all subfactors

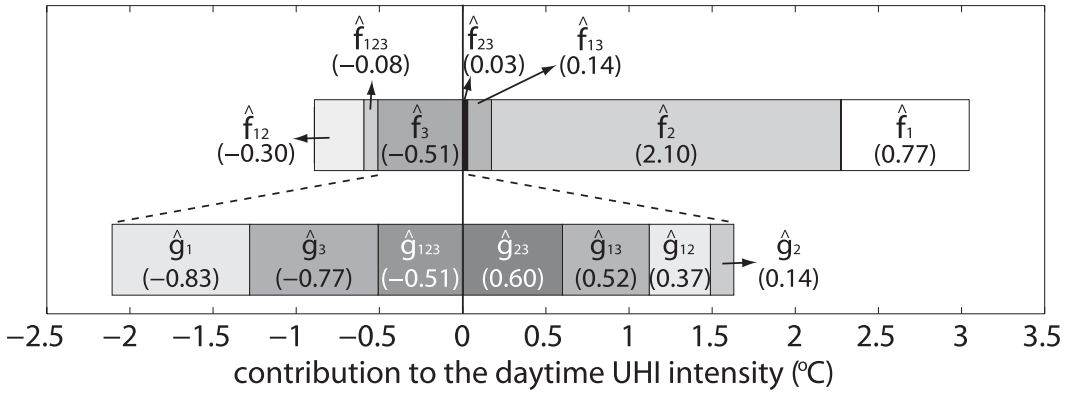

FIG. 1. Contributions of the factors and their interactions to the daytime UHI intensity. The units of the numbers in the parentheses are degrees Celsius.

(2003) who examined the effect of roughness length on the UHI intensity. Therefore, the air temperature near the surface (not the surface temperature) can decrease. The surface temperature and storage heat flux actually increase in the daytime when the G_3 factor is included. The subfactors interact considerably with each other. All of the interactions between two factors ($\hat{g}_{12}$, $\hat{g}_{13}$, and $\hat{g}_{23}$) contribute positively to the daytime UHI intensity. The contribution of the interaction between all three factors $\hat{g}_{123}$ is negative.

In the nighttime, the largest contribution to the UHI intensity comes from the anthropogenic heat (86%). As demonstrated in previous studies (Ichinose et al. 1999; Fan and Sailor 2005), the contribution of the anthropogenic heat is much larger in the nighttime than in the daytime. The second most important factor is the impervious-surfaces factor, leading to a contribution of 47%. The 3D urban geometry contributes positively to the nighttime UHI intensity (28%). Unlike the F_1 and F_2 factors, the F_3 factor displays contrasting effects on the daytime and nighttime UHI intensities. That is, the 3D urban geometry factor decreases the UHI intensity in the daytime but increases it in the nighttime. There are numerous observational studies that have investigated the relationship between urban geometry that can be represented by canyon aspect ratio [height-to-width (H/W) ratio of an urban canyon] or sky-view factor and nighttime UHI intensities (e.g., Yamashita et al. 1986; Oke 1987; Giridharan et al. 2007). The general trend is that the nighttime UHI intensity increases with increasing building height or density. Although it is not straightforward to directly compare the pure contribution of the 3D urban geometry factor with its relationship with the UHI intensity, the result of the 3D urban geometry effect is consistent with that found in previous observational studies.

The contribution of the interaction between the anthropogenic heat and impervious-surfaces factors $\hat{f}_{12}$ is negative and large, and is almost one-half of $\hat{f}_1$ in magnitude. The interaction between the F_1 and F_3 factors $\hat{f}_{13}$ is also negative and large. The anthropogenic heat itself has a strong impact on the UHI intensity, especially in the nighttime. Only a part of the anthropogenic heat is used to heat the atmosphere when the F_1 factor is

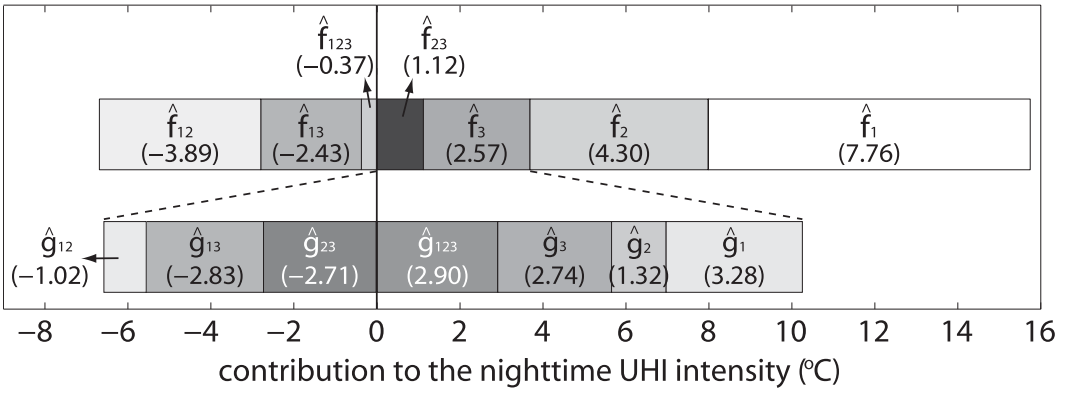

FIG. 2. As in Fig. 1, but for the nighttime UHI intensity.

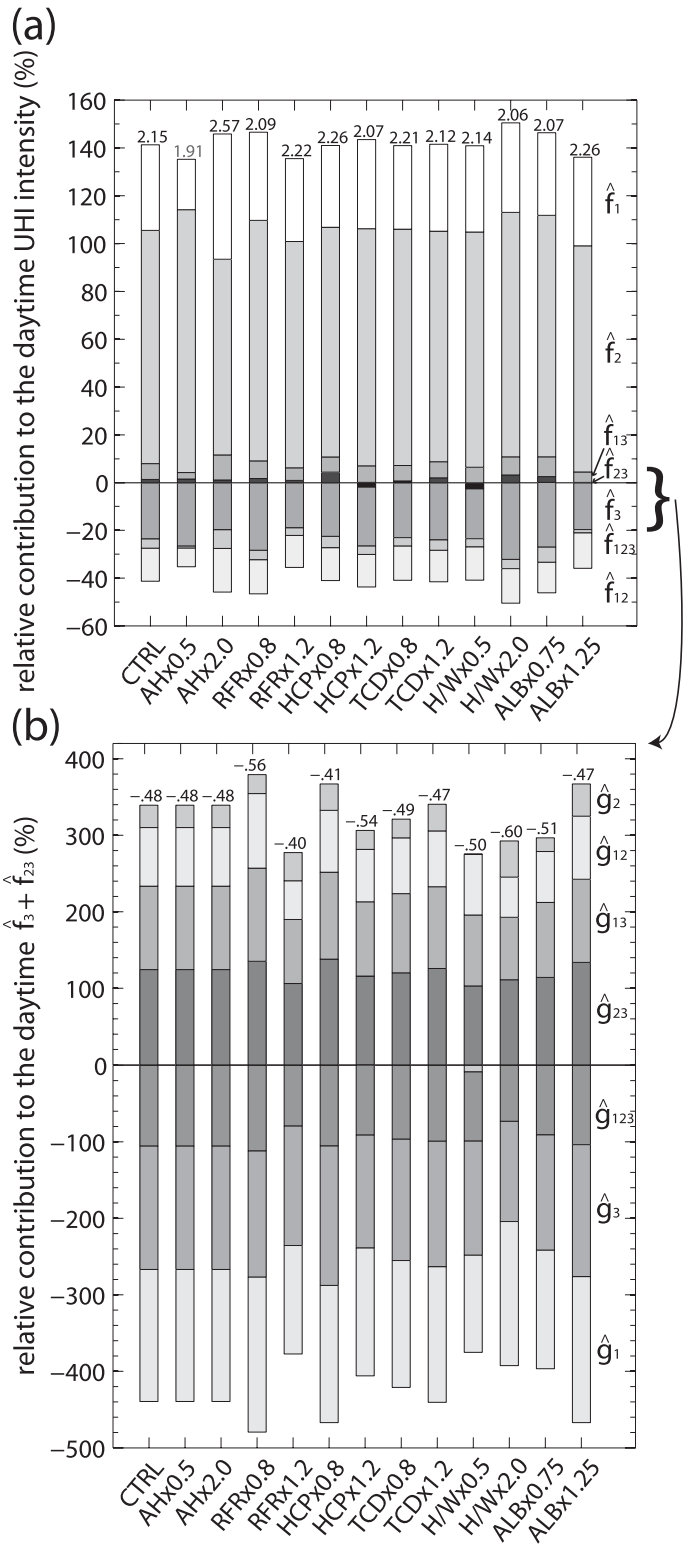

FIG. 3. Relative contributions of (a) the main factors and their interactions to the daytime UHI intensity and (b) the subfactors and their interactions to the daytime $\hat{f}_3 + \hat{f}_{23}$ for the control experiment (CTRL) and various sensitivity experiments. In the sensitivity experiments, for example, AH × 0.5 means the half–anthropogenic heat experiment and RFR × 0.8 means the experiment with a roof fraction reduced by 20% from the value used in CTRL. The description of the sensitivity experiments is given in the text and Table 2. Note that in the sensitivity experiments each parameter value varies while other parameter values remain the same as those in CTRL. The numbers above the bars indicate the sum of all contributions, and the units of the numbers are degrees Celsius.

accompanied by other factors, however, because it interacts strongly with other factors, giving the negative contributions. Hence, the difference in the nighttime average temperature between the f_{123} and f_{23} experiments that correspond to the experiments with and without the anthropogenic heat, respectively, and that include the effects of the other factors is only 1.07°C. This difference is consistent with the results of previous studies (Ichinose et al. 1999; Fan and Sailor 2005) that indicate an ~1°C contribution of anthropogenic heat to the summer nighttime UHI intensity when comparing experiments with and without anthropogenic heat. Whereas the interactions between the anthropogenic heat and other factors ($\hat{f}_{12}$ and $\hat{f}_{13}$) contribute negatively to the nighttime UHI intensity, the interaction between the F_2 and F_3 factors ($\hat{f}_{23}$) contributes positively by 12%. The contribution of the interaction among all three factors is −4%.

The 3D urban geometry contributes considerably to the nighttime UHI intensity ($\hat{f}_3 = 2.57$°C). Among the three subfactors, the G_1 factor plays the most important role in the nighttime UHI intensity ($\hat{g}_1 = 3.28$°C). This means that in the nighttime a large amount of heat is released from the vertical walls. From the G_1 effect, increased warming due to the walls will likely occur with increasing building height, thus causing a nighttime thermal environment in urban areas to deteriorate. The radiation trapping contributes positively ($\hat{g}_2 = 1.32$°C). We first expected that longwave radiation trapping dominates this positive contribution, but the net longwave radiation in the g_2 experiment decreases by 7.1 W m^{-2} as compared with that in the g_0 experiment. This is due to the increase in the surface temperatures within the urban canyon resulting from the enhanced absorption of shortwave radiation in the daytime. Thus, although longwave radiation trapping occurs within the urban canyon, the net longwave radiation decreases in the g_2 experiment. In the g_3 experiment, because of the large storage heat in the daytime, the surface temperatures still remain high enough to yield weak but positive sensible heat fluxes from the urban canyon and from the roof ($\hat{g}_3 = 2.74$°C). In the nighttime, the contributions of the interactions between the subfactors are as large as in the daytime. Therefore, it is concluded that not only the subfactors themselves but also the complex interactions between the subfactors contribute significantly to the 3D urban geometry effect.

b. Sensitivity experiments

In this section, we examine the sensitivities of the relative contributions of the factors and their interactions to anthropogenic heat intensity and various urban surface parameters. Figures 3 and 4 show the relative contributions of the factors and their interactions to the daytime and nighttime UHI intensities, respectively. The relative contribution is calculated by dividing each contribution by the sum of all contributions for each experiment.

In the half–anthropogenic heat experiment (denoted by AH × 0.5), the daytime and nighttime UHI intensities are reduced by 0.24° and 0.46°C, respectively, as compared with those in the control experiment. The contribution of the anthropogenic heat factor $\hat{f}_1$ to the daytime (nighttime) UHI intensity decreases to 21% (74%) from 36% (86%) of the control experiment. The other contributions are also altered. For example, the contribution of the impervious-surfaces factor $\hat{f}_2$ to the daytime (nighttime) UHI intensity increases to 110% (50%). In the double–anthropogenic heat experiment (denoted by AH × 2.0), however, $\hat{f}_1$ increases to 52% in the daytime and to 87% in the nighttime and $\hat{f}_2$ decreases to 82% in the daytime and to 43% in the nighttime. These results indicate that the relative contribution of the anthropogenic heat factor to the UHI intensity depends to some extent on the anthropogenic heat intensity.

The roof fraction is the ratio of the building (roof) area to the built-up area in the urban area. So, the urban-averaged energy fluxes reflect the effects of the buildings (urban canyon) more as the roof fraction increases (decreases). Because most of the physical processes associated with the 3D urban geometry factor occur within the urban canyon, the relative contributions of the 3D urban geometry factor to the daytime and nighttime UHI intensities increase as the urban canyon fraction increases (or the roof fraction decreases). As a result, $\hat{f}_3$ increases in magnitude by 9% (8%) in the daytime (nighttime) when the roof fraction decreases to 0.4 (RFR × 0.8) from 0.6 (RFR × 1.2). Likewise, the daytime UHI intensity decreases but the nighttime UHI intensity increases as the urban canyon fraction increases because $\hat{f}_3$ is negative in the daytime and positive in the nighttime.

As the heat capacity increases, more heat can be stored in the urban fabrics. The differences in the daytime and nighttime $\hat{f}_2$ are 3% and 9%, respectively, when the heat capacities of the surfaces increase to 1.68 MJ m^{-3} K^{-1} (HCP × 1.2) from 1.12 MJ m^{-3} K^{-1} (HCP × 0.8). In addition, the relative contribution of the interaction between the anthropogenic heat and impervious-surfaces factors $\hat{f}_{12}$ differs by 9% in the nighttime between the HCP × 0.8 and HCP × 1.2 experiments, which contributes negatively to the nighttime UHI intensity. The nighttime UHI intensity varies insignificantly in these experiments.

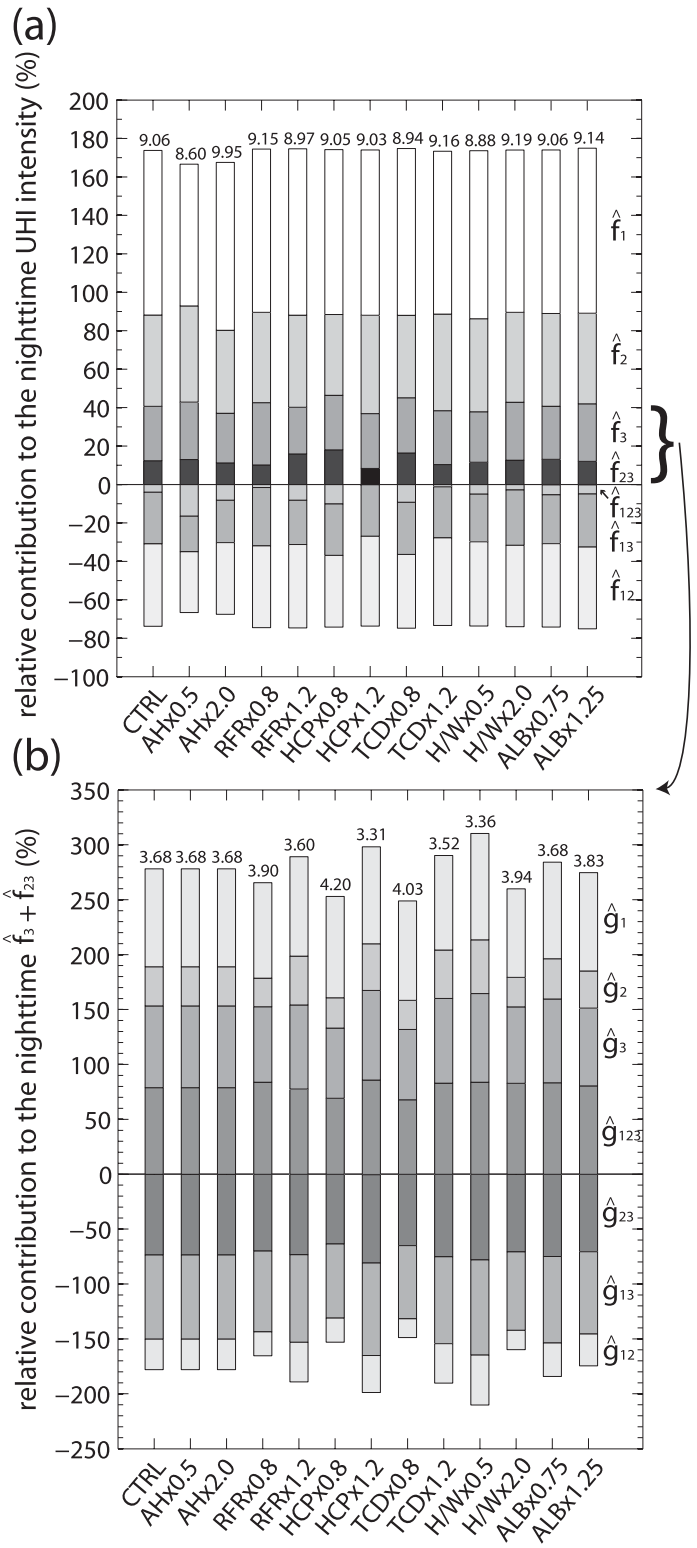

FIG. 4. As in Fig. 3, but for the nighttime UHI intensity.

As in the sensitivity experiments on heat capacity, the thermal conductivity is positively correlated with the impervious-surfaces effect. The difference in the nighttime $\hat{f}_2$ between the TCD $\times$ 0.8 and TCD $\times$ 1.2 experiments is 7%, whereas that in the daytime $\hat{f}_2$ is small (2%). In the nighttime, the contributions related to the impervious-surfaces factor ($\hat{f}_{12}$, $\hat{f}_{23}$, and $\hat{f}_{123}$) change considerably between the TCD $\times$ 0.8 and TCD $\times$ 1.2 experiments. The thermal conductivity influences the nighttime UHI intensity, indicating a decrease of 0.08°C in the TCD $\times$ 0.8 experiment and an increase of 0.1°C in the TCD $\times$ 1.2 experiment as compared with that in the control experiment.

The canyon aspect ratio (H/W) reflects the relative weight of the vertical surface area in the 3D urban geometry. So, one can expect that the contribution of the 3D urban geometry factor increases as the canyon aspect ratio increases. The $\hat{f}_3$ indicates increases of 11% and 4% in the daytime and nighttime, respectively, in magnitude between the $H/W \times 0.5$ and $H/W \times 2.0$ experiments. The $\hat{g}_1$ points to a significant increase in the daytime. Of interest is that $\hat{g}_2$ is negative in the $H/W \times 0.5$ experiment, unlike in the other experiments. When the canyon aspect ratio is small, the radiation-trapping effect can be relatively small but the shadow effect can play an important role in the radiation process. The nighttime UHI intensity increases with increasing canyon aspect ratio. In addition, the sum of all contributions of the subfactors and interactions increases as the canyon aspect ratio increases. This implies that the contribution of the 3D urban geometry factor becomes more important as the canyon aspect ratio increases.

The surface albedo is an important parameter in a thermal environment in urban areas. If one considers a special surface (e.g., white roof or wall) and assumes a very high surface albedo, the impact of surface albedo on UHI would be very large. In this study, a typical range of surface albedo (0.12–0.20) is considered, however. Under this range, the impact of surface albedo on the nighttime UHI intensity is small even though that on the daytime UHI intensity is considerable.

In summary, the relative contributions of the factors and their interactions vary to some extent depending on the anthropogenic heat intensity and the values of the urban surface parameters. Nonetheless, the deviation of the relative contributions in the sensitivity experiments from those in the control experiment is around 10% in general. The relative importance and ranking order of the contributions of the factors and interactions in the sensitivity experiments are similar to those in the control experiment.

4. Summary and conclusions

The relative contributions of the causative factors and their interactions to the daytime and nighttime UHI intensities were examined under an idealized urban environment. The main factors responsible for the UHI are anthropogenic heat, impervious surfaces, and three-dimensional urban geometry. In this study, the 3D urban geometry effect was explicitly examined using the urban canopy model. The 3D urban geometry factor is subdivided into three subfactors: additional heat stored in vertical walls, radiation trapping, and wind speed reduction, each arising from the distinctive geometry of cities. By performing a factor separation analysis, the contributions of the factors and their interactions are quantified.

The relative importance and ranking order of the factors and their interactions were found to differ between the daytime and nighttime. In the daytime, the impervious surfaces have the greatest effect on the UHI intensity (98%). The anthropogenic heat also contributes positively to the daytime UHI intensity (36%), but the 3D urban geometry contributes negatively to the daytime UHI intensity (−24%). Among the 3D urban geometry subfactors, the additional heat stored in vertical walls gives the largest negative contribution to the daytime UHI intensity. Because of shortwave radiation trapping within the urban canyon, the radiation trapping contributes positively to the daytime UHI intensity. The wind speed reduction resulting from the existence of buildings decreases the daytime UHI intensity. In the nighttime, the anthropogenic heat is crucial to the UHI intensity (86%), but this factor interacts strongly with other factors. The second most important contributing factor is the impervious-surfaces factor (47%). The nighttime contribution of the 3D urban geometry factor contrasts with the daytime contribution by yielding the positive contribution (28%). Among the 3D urban geometry subfactors, the additional heat stored in vertical walls contributes most to the nighttime UHI intensity and the radiation trapping and the wind speed reduction also contribute positively to that. We suggest that the 3D urban geometry effect should be included when considering the urban-related phenomena.

Through sensitivity experiments, it was found that the 3D urban geometry effect increases with increasing urban canyon fraction and canyon aspect ratio, thus possibly causing a nighttime thermal environment in urban areas to deteriorate. The sensitivity experiments indicated that although each of the contributions varies with the anthropogenic heat intensity and the values of the urban surface parameters, the relative importance and ranking order of the contributions are not significantly changed.

In this study, the relative contributions of the causative factors and the sensitivities to the intrinsic characteristics of the city were examined for a midlatitude city and summertime conditions. The relative contributions of the causative factors could differ depending on season, surrounding environment, city location, and meteorological conditions. For future studies, it is of interest to examine the effects of season (e.g., wintertime conditions), surrounding environment (e.g., soil properties and land-use/land-cover types of rural areas), city location (e.g., latitude), and meteorological conditions (e.g., wind speed) on the relative contributions of the causative factors.

Acknowledgments. The authors are grateful to three anonymous reviewers for providing valuable comments on this work. This work was supported by a National Research Foundation of Korea (NRF) grant funded by the Korea Ministry of Education, Science and Technology (MEST) (2011-0017041) and also by the Brain Korea 21 Project (through the School of Earth and Environmental Sciences, Seoul National University).

REFERENCES

Arnfield, A. J., 1982: An approach to the estimation of the surface radiative properties and radiation budgets of cities. *Phys. Geogr.,* **3,** 97–122.

——, 2003: Two decades of urban climate research: A review of turbulence, exchanges of energy and water, and the urban heat island. *Int. J. Climatol.,* **23,** 1–26.

Atkinson, B. W., 2003: Numerical modelling of urban heat-island intensity. *Bound.-Layer Meteor.,* **109,** 285–310.

Bottyan, Z., and J. Unger, 2003: A multiple linear statistical model for estimating the mean maximum urban heat island. *Theor. Appl. Climatol.,* **75,** 233–243.

Bowler, D. E., L. Buyung-Ali, T. M. Knight, and A. S. Pullin, 2010: Urban greening to cool towns and cities: A systematic review of the empirical evidence. *Landscape Urban Plann.,* **97,** 147–155.

Chen, F., and J. Dudhia, 2001: Coupling an advanced land surface–hydrology model with the Penn State–NCAR MM5 modeling system. Part I: Model implementation and sensitivity. *Mon. Wea. Rev.,* **129,** 569–585.

Chen, S.-H., and W.-Y. Sun, 2002: A one-dimensional time dependent cloud model. *J. Meteor. Soc. Japan,* **80,** 99–118.

Dudhia, J., 1989: Numerical study of convection observed during the winter monsoon experiment using a mesoscale two-dimensional model. *J. Atmos. Sci.,* **46,** 3077–3107.

Dupont, S., and P. G. Mestayer, 2006: Parameterization of the urban energy budget with the submesoscale soil model. *J. Appl. Meteor. Climatol.,* **45,** 1744–1765.

Fan, H., and D. J. Sailor, 2005: Modeling the impacts of anthropogenic heating on the urban climate of Philadelphia: A comparison of implementations in two PBL schemes. *Atmos. Environ.,* **39,** 73–84.

Fung, W. Y., K. S. Lam, J. Nichol, and M. S. Wong, 2009: Derivation of nighttime urban air temperatures using a satellite thermal image. *J. Appl. Meteor. Climatol.,* **48,** 863–872.

Gedzelman, S. D., S. Austin, R. Cermak, N. Stefano, S. Partridge, S. Quesenberry, and D. A. Robinson, 2003: Mesoscale aspects of the urban heat island around New York City. *Theor. Appl. Climatol.,* **75,** 29–42.

Giridharan, R., S. S. Y. Lau, S. Ganesan, and B. Givoni, 2007: Urban design factors influencing heat island intensity in high-rise high-density environments of Hong Kong. *Build. Environ.,* **42,** 3669–3684.

——, ——, ——, and ——, 2008: Lowering the outdoor temperature in high-rise high-density residential developments of coastal Hong Kong: The vegetation influence. *Build. Environ.,* **43,** 1583–1595.

Grimmond, C. S. B., 2007: Urbanization and global environmental change: Local effects of urban warming. *Geogr. J.,* **173,** 83–88.

Hidalgo, J., V. Masson, A. Baklanov, G. Pigeon, and L. Gimeno, 2008: Advances in urban climate modeling. *Ann. N. Y. Acad. Sci.,* **1146,** 354–374.

Hong, S.-Y., Y. Noh, and J. Dudhia, 2006: A new vertical diffusion package with an explicit treatment of entrainment processes. *Mon. Wea. Rev.,* **134,** 2318–2341.

Ichinose, T., K. Shimodozono, and K. Hanaki, 1999: Impact of anthropogenic heat on urban climate in Tokyo. *Atmos. Environ.,* **33,** 3897–3909.

Johnson, G. T., T. R. Oke, T. J. Lyons, D. G. Steyn, I. D. Watson, and J. A. Voogt, 1991: Simulation of surface urban heat islands under ''ideal'' conditions at night. Part 1: Theory and tests against field data. *Bound.-Layer Meteor.,* **56,** 275–294.

Kim, Y.-H., and J.-J. Baik, 2002: Maximum urban heat island intensity in Seoul. *J. Appl. Meteor.,* **41,** 651–659.

——, and ——, 2004: Daily maximum urban heat island intensity in large cities of Korea. *Theor. Appl. Climatol.,* **79,** 151–164.

Klysik, K., and K. Fortuniak, 1999: Temporal and spatial characteristics of the urban heat island of Lodz, Poland. *Atmos. Environ.,* **33,** 3885–3895.

Kondo, H., and Y. Kikegawa, 2003: Temperature variation in the urban canopy with anthropogenic energy use. *Pure Appl. Geophys.,* **160,** 317–324.

Kruger, E. L., F. O. Minella, and F. Rasia, 2011: Impact of urban geometry on outdoor thermal comfort and air quality from field measurements in Curitiba, Brazil. *Build. Environ.,* **46,** 621–634.

Kusaka, H., and F. Kimura, 2004: Thermal effects of urban canyon structure on the nocturnal heat island: Numerical experiment using a mesoscale model coupled with an urban canopy model. *J. Appl. Meteor.,* **43,** 1899–1910.

——, H. Kondo, Y. Kikegawa, and F. Kimura, 2001: A simple single-layer urban canopy model for atmospheric models: Comparison with multi-layer and slab models. *Bound.-Layer Meteor.,* **101,** 329–358.

Lee, S.-H., C.-K. Song, J.-J. Baik, and S.-U. Park, 2009: Estimation of anthropogenic heat emission in the Gyeong-In region of Korea. *Theor. Appl. Climatol.,* **96,** 291–303.

Martilli, A., 2002: Numerical study of urban impact on boundary layer structure: Sensitivity to wind speed, urban morphology, and rural soil moisture. *J. Appl. Meteor.,* **41,** 1247–1266.

——, A. Clappier, and M. W. Rotach, 2002: An urban surface exchange parameterisation for mesoscale models. *Bound.-Layer Meteor.,* **104,** 261–304.

Masson, V., 2000: A physically-based scheme for the urban energy budget in atmospheric models. *Bound.-Layer Meteor.,* **94,** 357–397.

Mills, G., 1997: An urban canopy-layer climate model. *Theor. Appl. Climatol.,* **57,** 229–244.

Mirzaei, P. A., and F. Haghighat, 2010: Approaches to study urban heat island—Abilities and limitations. *Build. Environ.,* **45,** 2192–2201.

Mlawer, E. J., S. J. Taubman, P. D. Brown, M. J. Iacono, and S. A. Clough, 1997: Radiative transfer for inhomogeneous atmospheres: RRTM, a validated correlated-*k* model for the longwave. *J. Geophys. Res.,* **102,** 16 663–16 682.

Morris, C. J. G., I. Simmonds, and N. Plummer, 2001: Quantification of the influences of wind and cloud on the nocturnal urban heat island of a large city. *J. Appl. Meteor.,* **40,** 169–182.

Ohashi, Y., Y. Genchi, H. Kondo, Y. Kikegawa, H. Yoshikado, and Y. Hirano, 2007: Influence of air-conditioning waste heat on air temperature in Tokyo during summer: Numerical experiments using an urban canopy model coupled with a building energy model. *J. Appl. Meteor. Climatol.,* **46,** 66–81.

Oke, T. R., 1981: Canyon geometry and the nocturnal urban heat island: Comparison of scale model and field observations. *J. Climatol.,* **1,** 237–254.

——, 1982: The energetic basis of the urban heat island. *Quart. J. Roy. Meteor. Soc.,* **108,** 1–24.

——, 1987: *Boundary Layer Climates*. 2nd ed. Routledge, 435 pp.

Rizwan, A. M., L. Y. C. Dennis, and C. Liu, 2008: A review on the generation, determination and mitigation of Urban Heat Island. *J. Environ. Sci.,* **20,** 120–128.

Runnalls, K. E., and T. R. Oke, 2000: Dynamics and controls of the near-surface heat island of Vancouver, British Columbia. *Phys. Geogr.,* **21,** 283–304.

Ryu, Y.-H., J.-J. Baik, and S.-H. Lee, 2011: A new single-layer urban canopy model for use in mesoscale atmospheric models. *J. Appl. Meteor. Climatol.,* **50,** 1773–1794.

Shahmohamadi, P., A. I. Che-Ani, A. Ramly, K. N. A. Maulud, and M. F. I. Mohd-Nor, 2010: Reducing urban heat island effects: A systematic review to achieve energy consumption balance. *Int. J. Phys. Sci.,* **5,** 626–636.

Skamarock, W. C., and Coauthors, 2008: A description of the Advanced Research WRF version 3. NCAR Tech. Note NCAR/TN-475+STR, 113 pp.

Stein, U., and P. Alpert, 1993: Factor separation in numerical simulations. *J. Atmos. Sci.,* **50,** 2107–2115.

Taha, H., 1997: Urban climates and heat islands: Albedo, evapotranspiration, and anthropogenic heat. *Energy Build.,* **25,** 99–103.

——, H. Akbari, A. Rosenfeld, and J. Huang, 1988: Residential cooling loads and the urban heat island—The effects of albedo. *Build. Environ.,* **23,** 271–283.

Terjung, W. H., and S. S.-F. Louie, 1973: Solar radiation and urban heat islands. *Ann. Assoc. Amer. Geogr.,* **63,** 181–207.

Tokairin, T., H. Kondo, H. Yoshikado, Y. Genchi, T. Ihara, Y. Kikegawa, Y. Hirano, and K. Asahi, 2006: Numerical study on the effect of buildings on temperature variation in urban and suburban areas in Tokyo. *J. Meteor. Soc. Japan,* **84,** 921–937.

Velazquez-Lozada, A., J. E. Gonzalez, and A. Winter, 2006: Urban heat island effect analysis for San Juan, Puerto Rico. *Atmos. Environ.,* **40,** 1731–1741.

Yamashita, S., K. Sekine, M. Shoda, K. Yamashita, and Y. Hara, 1986: On relationships between heat island and sky view factor in the cities of Tama River basin, Japan. *Atmos. Environ.,* **20,** 681–686.

Zoulia, I., M. Santamouris, and A. Dimoudi, 2009: Monitoring the effect of urban green areas on the heat island in Athens. *Environ. Monit. Assess.,* **156,** 275–292.